Aragonitic rostra of the Turonian belemnitid *Goniocamax*: Arguments from diagenesis

YANNICKE DAUPHIN, C. TERRY WILLIAMS, and IGOR S. BARSKOV

Dauphin, Y., Williams, C.T., and Barskov, I.S. 2007. Aragonitic rostra of the Turonian belemnitid *Goniocamax*: Arguments from diagenesis. *Acta Palaeontologica Polonica* 52 (1): 85–97.

The hypothesis that belemnitid rostra are formed by primary biogenic low-Mg calcite is widespread. However, the coexistence in the same rostrum of both aragonitic and calcitic components has been reported in true belemnites (*Goniocamax*, Turonian). A combined microstructural and chemical composition study of the comparison of shells with undisputed mineralogy from the same site as the Turonian *Goniocamax*, shows that these aragonitic shells display the effects of diagenetic alteration. These observations favour the hypothesis that belemnite rostra are composed of primary aragonite, rather than low-Mg calcite, and are consistent with all other cephalopod shells. Calcitic and aragonitic rostra are also known in other Dibranchiata such as Triassic Aulacocerida and Eocene *Belopterina*. Diagenetic changes such as shown here may clearly affect palaeo-environmental interpretations based on carbonate shells.

Key words: Cephalopoda, Belemnitida, *Goniocamax*, palaeo-environment, aragonite, calcite, diagenesis, Turonian, Piasina River, Siberia.

Yannicke Dauphin [yannicke.dauphin@u-psud.fr], UMR IDES du CNRS, bat 504, Université Paris XI-Orsay, F-91405 Orsay Cedex, France;
C.T. Williams [ctw@nhm.ac.uk], Department of Mineralogy, Natural History Museum, Cromwell Road, London, SW7 5BD, United Kingdom;
I.S. Barskov, Department of Paleontology, Geological Faculty, Moscow State University, 119899 Moscow GSP V-234, Russia.

Introduction

Diagenetic alteration of biogenic carbonate, resulting from burial or fossilisation processes, can play a significant role in many aspects of systematic and palaeo-environmental studies involving marine or freshwater shells. The application of advanced microstructural and biogeochemical techniques now employed in palaeontology requires a clear understanding of the effects of diagenesis on the microstructures themselves, and on the organic and inorganic components in the shells. Whilst there is a growing body of information on the processes affecting mammalian or reptilian apatitic bone during fossilisation, diagenetic alteration of biogenic calcite and aragonite is less well studied.

Belemnites (or belemnoids) are an extinct group of marine cephalopods that proliferated in the Jurassic and Cretacous periods. Belemnites had an internal skeleton comprising a *rostrum* (the most commonly preserved part of the skeleton) connected to a thin-walled chambered *phragmocone* (sometimes preserved), that projects towards the anterior as the *pro-ostracum* (only rarely preserved, e.g., Doguzhaeva et al. 2003).

For some thirty years, it was generally believed that belemnitid rostra were composed of primary biogenic low-Mg calcite, in contrast to other Recent and fossil cephalopod shells that are composed of primary aragonite. Thus, when "belemnitid rostra" composed of aragonite were first discovered, these specimens were excluded from the Belemnitida, and new taxa were created (Makowski 1962; Jeletzky 1966; Reitner and Engeser 1982; Engeser and Reitner 1983). Unfortunately, few of these earlier studies provided information on the microstructures and the chemical composition of these aragonite rostra, in part because of the rarity of the specimens prohibited the use of "destructive" analytical techniques that were the only available at that time. Spaeth (1971) described aragonitic rostral layers in *Neohibolites*, but no analytical data were provided. Spaeth also compared the alveolar structure of the rostra of *Neohibolites* to the ventral part of the *Sepia* shell, but the ventral part of *Sepia* is homologous of the phragmocone (Barskov 1972, 1973).

There are currently four hypotheses relating to the nature of belemnitid rostra: (1) they are composed of primary calcite, (2) they are composed of primary aragonite, (3) they are completely organic in composition (Muller-Stoll 1936), (4) the juvenile rostrum is composed of aragonite, the adult rostrum is calcitic (Bandel et al. 1984). It has not yet been fully resolved as to which of these hypotheses is correct. Nevertheless, proposals on homologies of Recent and fossil cephalopod should rely on microstructural and mineralogical data (Barskov 1972, 1973; Dauphin 1983).

Diagenetic processes include both the burial environment and subsequent history of the sediments, and these can all alter to varying degrees the composition, the mineralogy, and

structure of biogenic carbonates. Such alterations can be unpredictable, e.g., some specimens of Triassic *Aulacoceras* are preserved in calcite, whereas others as aragonite (Cuif et al. 1977; Dauphin and Cuif 1980; Dauphin 1987). Similar preservation of Eocene *Belopterina* has been described (Dauphin 1986, 1988), but these genera are not "true" Belemnitida (Jeletzky 1966). Teys et al. (1978) provided the first description of the coexistence of aragonite and calcite components within the same rostrum. These exceptional samples with rostrum and phragmocone have been described as *Goniocamax*, and are true Belemnitida (Naydin et al. 1987; Barskov et al. 1997). *Goniocamax* Naydin, 1964, was first described as a subgenus of *Gonioteuthis* (Belemnopseina, Bellemnitellidae). The status of the genus and related species are under discussion (Kostak et al. 2004).

Stable isotope data have distinguished two groups of fossil shells: belemnitids and bivalves (with the exception of inoceramids) that have relatively high $\delta^{18}O$ values, whereas gastropods and inoceramids have lower values (Teys et al. 1978; Naydin et al. 1987). In the aragonite and calcite sections of *Goniocamax*, the ^{13}C contents differ but the ^{18}O contents are similar. From microstructural information, the aragonite components of the gastropod and bivalve shells show the effects of some diagenetic changes (Barskov et al. 1997), however, the compositions of the fossils from this site are unknown. In this report, we describe the compositional changes that have occurred during the fossilisation of the mollusc shells, and we attempt to link these changes to those observed in the microstructure of the shells. Implications for palaeo-environmental reconstructions are briefly discussed.

Institutional abbreviation.—UPS, Université Paris XI, France.

Materials and methods

Materials.—*Goniocamax* rostra were collected from calcareous nodules in "sands with layers of sandstones, siltstones, and clays" from the Turonian of Northern Siberia (Piasina River, Western Taymyr Peninsula). The maximum diameter of the five samples studied is less than 1 cm, and the maximum length is ~2 cm (Fig. 1A, B) (Teys et al. 1978). X-ray structural data show that the anterior part of the rostrum is composed of aragonite, whereas the posterior part is calcite. Of the five samples studied, all underwent microstructural examination, quantitative chemical analyses were undertaken on three samples, and one was for element maps. Other molluscan shells were observed from this site, with inoceramids, gastropods and ammonites being the most abundant, as well as one thin *Pecten* shell.

Several species of Recent molluscs of related taxa and with similar microstructure were analysed as a comparison for the fossil samples. These samples were *Nautilus macromphalus*, *Sepia* sp., and *Spirula spirula* from New Caledonia; *Pinna nobilis* from the Mediterranean Sea (Port Cros Island), and *Pecten maximus* from Brittany. Because the small pieces of the fossil gastropod shells could not be identified in terms of their taxonomy, several Recent gastropods with aragonite crossed lamellar shells were analysed as a comparison: *Cypraea leviathan* from Tuamotu Islands; *Strombus gigas* from Caraibes; *Cerithium* sp., *Murex* sp., and *Natica* sp. of unknown origin. The nacreous layer of the outer wall of *Spirula* is very thin and poorly calcified, whereas that of *Sepia* is composed of two sub-layers, one of them being organic in composition (Dauphin 1981). The only well-developed shell layer in *Goniocamax* is the rostrum; thus the nacreous layers of the two Recent coleoid shells were not analysed.

Analytical methods.—A Cameca SX50 wavelength-dispersive electron microprobe at the Natural History Museum of London was used to obtain the compositions and elemental maps of the samples. For quantitative analysis, operating conditions used were 15 kV accelerating voltage and 20 nA specimen current, and for element maps a 100 nA specimen current was employed.

Additional data were obtained on an analytical scanning electron microscope (Philips 505 SEM) with an energy dispersive spectrometer (EDS). Quantitative analyses were obtained using a Link AN10000 ZAF/PB program that estimates peak-to-background ratios. The ZAF/PB method can be applied to specimens with rough surfaces, essential for the etched surfaces (see below). Small pieces of shell were em-

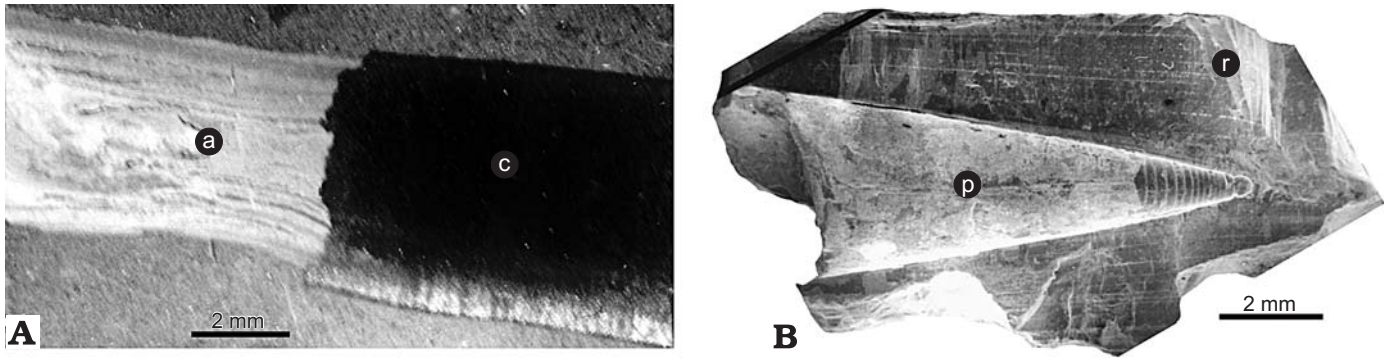

Fig. 1. Two SEM images illustrating different aspects of *Goniocamax* sp. from the Turonian of Northern Siberia, Piasina River, Western Taymyr Peninsula. **A**. UPS-1483, polished and etched longitudinal section of a rostrum showing the aragonitic region (a, white) and the calcitic region (c, black). **B**. UPS-2451, longitudinal fracture showing a part of the phragmocone (p) with some septa visible, and rostrum (r).

Table 1. Chemical composition (in ppm) of Recent shell layers. Abbreviations: m, mean; s, standard deviation; op, outer aragonitic layer; ip, inner aragonitic layer; nac, aragonitic nacreous layer; cl, aragonitic crossed lamellar layer of gastropods; fol, calcitic layer; *, EDS analyses; n.d., not detected.

			Na	Mg	P	S	Mn	Fe	Sr	Ca
Sepia	op	m	4340	n.d.	n.d.	n.d.	n.d.	n.d.	2673	395880
		s	211	–	–	–	–	–	616	4225
	ip	m	3125	n.d.	n.d.	n.d.	740	n.d.	2795	385110
		s	134	–	–	–	792	–	35	3253
Spirula	op	m	4947	n.d.	n.d.	n.d.	n.d.	n.d.	2533	387303
		s	159	–	–	–	–	–	491	1301
	ip	m	4733	743	n.d.	663	n.d.	n.d.	3177	389793
		s	501	–	–	–	–	–	198	4464
Nautilus	op	m	5340	n.d.	n.d.	n.d.	n.d.	n.d.	1850	380313
		s	95	–	–	–	–	–	323	9712
	nac	m	4947	n.d.	n.d.	n.d.	n.d.	n.d.	1724	370487
		s	116	–	–	–	–	–	446	8697
	ip	m	4360	n.d.	n.d.	n.d.	n.d.	n.d.	3183	387072
		s	434	–	–	–	–	–	388	2843
Pinna	nac	m	3117	n.d.	533	533	n.d.	n.d.	1233	398750
		s	995	–	308	–	–	–	367	5126
Gastropods	cl*	m	2223	n.d.	n.d.	n.d.	n.d.	n.d.	3888	324888
		s	360	–	–	–	–	–	657	12755
Pecten	fol*	m	5200	1600	800	2100	n.d.	n.d.	1200	394200
		s	1800	1300	400	800	–	–	500	12400

Table 2. Chemical composition (in ppm) of fossil shell layers, sedimentary calcite and sediment. Abbreviations: m, mean; s, standard deviation; op, outer aragonitic layer; ip, inner aragonitic layer; nac, aragonitic nacreous layer; cl, aragonitic crossed lamellar layer of gastropods; fol, calcitic layer; *, EDS analyses; LC, cross lamellar layers; n.d., not detected.

			Na	Mg	P	S	Mn	Fe	Sr	Ca
Goniocamax	op	m	1328	6739	n.d.	n.d.	n.d.	n.d.	2051	365950
		s	134	354	–	–	–	–	328	1271
	op	m	1154	n.d.	558	n.d.	n.d.	n.d.	5509	353412
		s	579	–	185	–	–	–	664	23217
	op*	m	2326	7605	882	n.d.	n.d.	1179	1877	395985
		s	1520	2020	1202	–	–	1332	597	18119
	op*	m	2406	521	1103	574	n.d.	1344	7027	395978
		s	1618	601	727	350	–	1325	1517	20594
	op*	m	1142	508	1158	958	n.d.	533	7983	312300
		s	1460	579	1192	433	–	515	1509	12625
	op*	m	1392	5885	n.d.	n.d.	n.d.	654	1777	321469
		s	1380	1362	–	–	–	521	277	14411
Ammonite	nac	m	2759	n.d.	n.d.	n.d.	n.d.	n.d.	4850	360441
		s	186	–	–	–	–	–	451	3462
	nac	m	3142	n.d.	528	n.d.	n.d.	n.d.	5512	360996
		s	302	–	162	–	–	–	829	2872
	ip	m	3247	n.d.	n.d.	n.d.	n.d.	n.d.	2325	373162
		s	384	–	–	–	–	–	621	1756
Inoceramids (fragments)	nac	m	2854	n.d.	649	n.d.	n.d.	n.d.	5676	370053
		s	815	–	567	–	–	–	4220	1825
Gastropods (fragments)	LC	m	2223	n.d.	n.d.	n.d.	n.d.	n.d.	3888	324888
		s	360	–	–	–	–	–	657	12755
Pecten	fol	m	903	917	n.d.	n.d.	n.d.	n.d.	717	384323
		s	391	6	–	–	–	–	309	1672
calcite		m	n.d.	12463	1137	n.d.	2707	9597	n.d.	352273
		s	140	1779	230	–	385	100	–	2258
sediment	*	m	15553	10507	28627	1440	3240	41667	5000	164813
		s	26298	13853	28945	3013	2403	31089	2143	108023

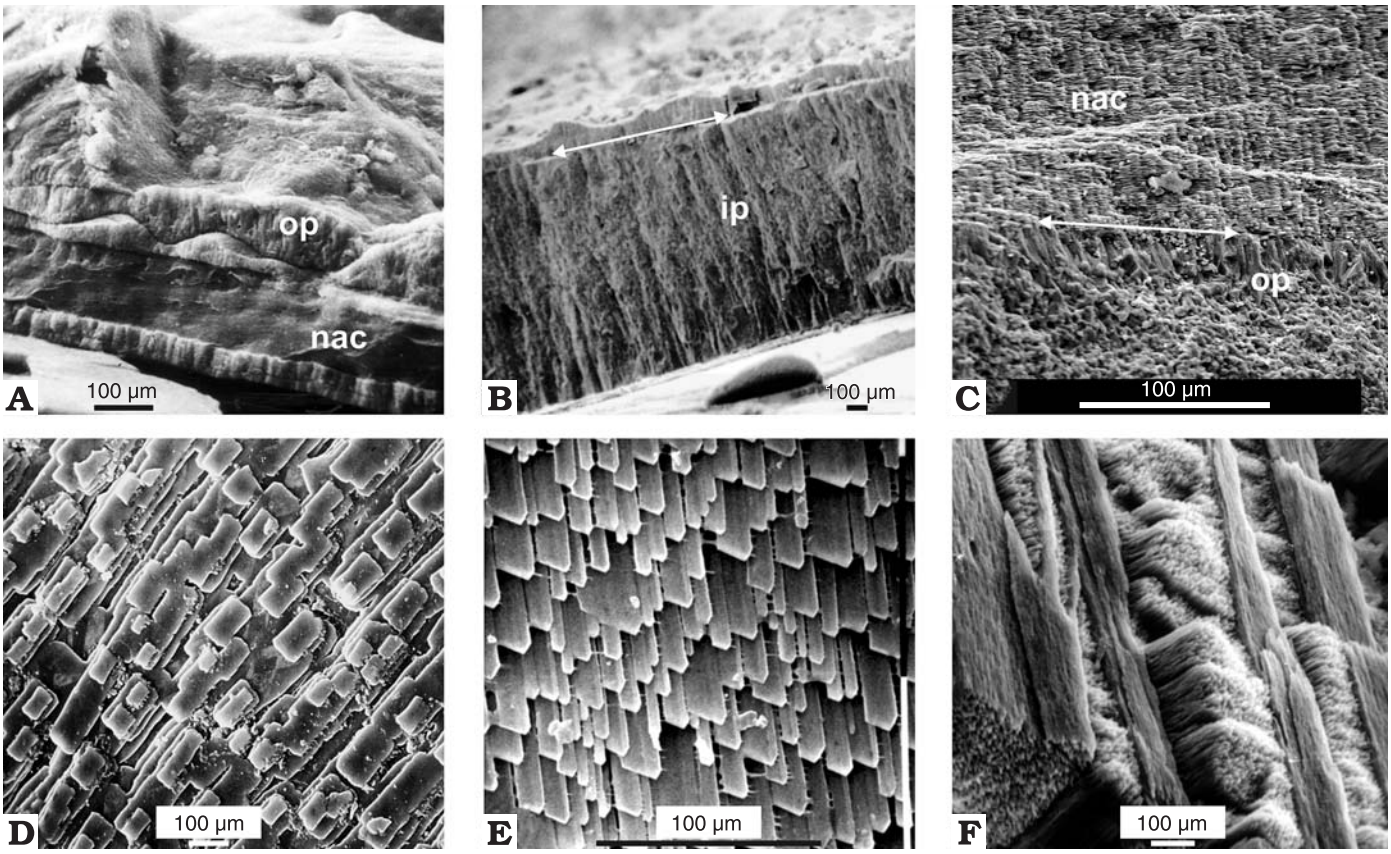

Fig. 2. Secondary electron images illustrating the microstructures of Recent shells. **A**. Dorsal shield of *Sepia* sp. (from New Caledonia), showing the thin inner prismatic layer, the nacreous layer and the thick multi-layered outer spherulitic prismatic layer. **B**. Outer wall of *Spirula* sp. (from New Caledonia), showing two prismatic layers and a mainly organic thin nacreous layer (arrow). **C**. *Nautilus macromphalus* (from New Caledonia). **D**. Nacreous layer of the pelecypod *Pinna nobilis* (from the Mediterranean Sea, Port Cros Island). **E**. Foliated calcite layer of *Pecten maximus* (from Brittany, France). **F**. Crossed lamellar aragonite layer of the gastropod *Murex* sp. (of unknown origin). Abbreviations: ip, inner prismatic layer; nac, nacreous layer; op, outer prismatic layer. All specimens from the UPS collection of Recent molluscs, not numbered.

bedded in an epoxy resin and polished using various grades of diamond paste. The polished surfaces were lightly etched in 5% formic acid for 15 sec to reveal microstructural details of the samples. The locations of the analysed points with respect to the structural features were therefore precisely known. Cobalt was used to provide the EDS calibration, and measurements were made using a live time of 100 or 200 sec with an accelerating voltage of 15 kV. The electron beam was optimised to achieve a small spot size that was estimated to have a diameter of 100 nm. The elements Na, Mg, P, S, Ca, Mn, Fe, and Sr were selected to illustrate aspects of shell composition. Several (>10) microprobe analyses were made at various locations on each sample, and analyses averaged to obtain an "individual" mean.

Statistical methods.—Although several microprobe analyses were made at various locations on individual shell layers, we have calculated the mean values as being representative of the sample. Thus, the standard deviations are higher than if they had been calculated from a number of spot analyses.

Some of the statistical tests could not be used in this study because the calculations of the averages given in Tables 1 and 2 have been derived using different procedures, a consequence of the rarity of the samples. For example, the average of the crossed lamellar layer of the Recent gastropods (Table 1) was calculated from five different species, because the fossil gastropod could not be identified at the species level. The average of the Recent *Pecten* was calculated from several specimens (>10). In contrast, the averages of the fossil *Pecten* or gastropod samples were based on individual analyses of a single specimen. Because of such disparities, parametric statistical tests were not used to estimate the differences in the chemical compositions, and notched box and whisker plots were used instead. In these plots, the central box covers the middle 50% of the data values, between the lower and upper quartiles. The «whiskers» extend out to the extreme (minimum and maximum values), while the central line is at the median. Anomalous values are plotted as separate points, and the whiskers extend only to those points that are within 1.5 times the interquartile range. A notch is added to each box corresponding to the width of a confidence interval for the median, while the width of the box is proportional to the square root of the number of observations in the data set. The confidence level on the notches is set to allow comparisons to be made at the 95% level by examining whether two notches overlap.

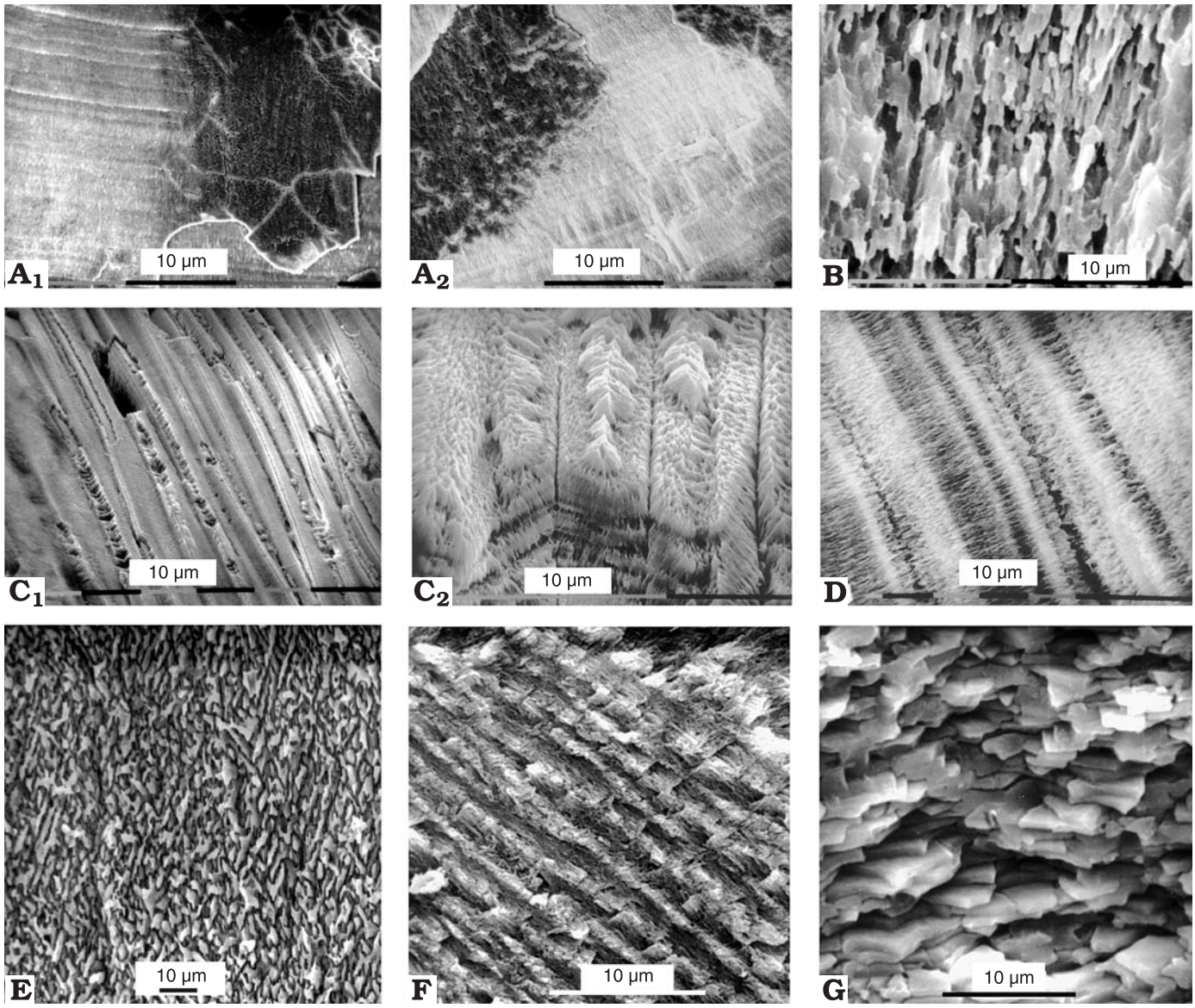

Fig. 3. Secondary electron images illustrating the microstructures in *Goniocamax* sp. (**A**–**D**) and fossil molluscs (**E**–**G**); all samples from the Turonian of N Siberia. **A**. UPS-2435, adjacent calcitic and aragonitic zones; the growth lines are not clearly visible in the calcitic zones. **B**. UPS-2460, non-compact, thin calcite prisms. **C**. UPS-2459, aragonitic sectors with preserved growth lines. **D**. UPS-2460, growth lines in the well-preserved aragonite. **E**. UPS-2448, aragonite nacreous of an ammonite shell. **F**. UPS-2591, crossed lamellar layer of a fossil gastropod. **G**. UPS-2587, nacreous layer of an inoceramid shell.

Only those elements with concentrations above the detection limit of the microprobe were used. Multivariate analyses (principal component analyses) were based on correlation matrices, so that the statistical weights of elements with high concentrations (i.e., Ca) were moderated within the software. The concentrations of elements were assigned as the variables, and the shell layers to individuals.

Results

Microstructural data

Recent samples.—The microstructures of the aragonite shells of *Nautilus*, *Spirula*, and *Sepia* have been described in detail (Mutvei 1964; Barskov 1972, 1973; Dauphin 1976). These shells are composed of three layers: an outer (spherulitic) prismatic layer (op), a middle nacreous layer (nac) and an inner prismatic layer (ip). The thickness and the degree of mineralisation of these three layers are different for each of the genera (Fig. 2A–C), being very thin in the outer wall of *Spirula*, whereas the nacreous layer is relatively thick and well mineralised in *Nautilus*. The dorsal shield of *Sepia* is entirely organic in the lateral parts of the shell, and subdivided into two layers in the middle section: the outer section being mineralised, and the inner section organic in composition.

Of the other samples studied, the shell of *Pinna* is composed of a thin inner nacreous layer (Fig. 2D), and a thicker calcite prismatic layer (Cuif et al. 1980, 1983); the calcite

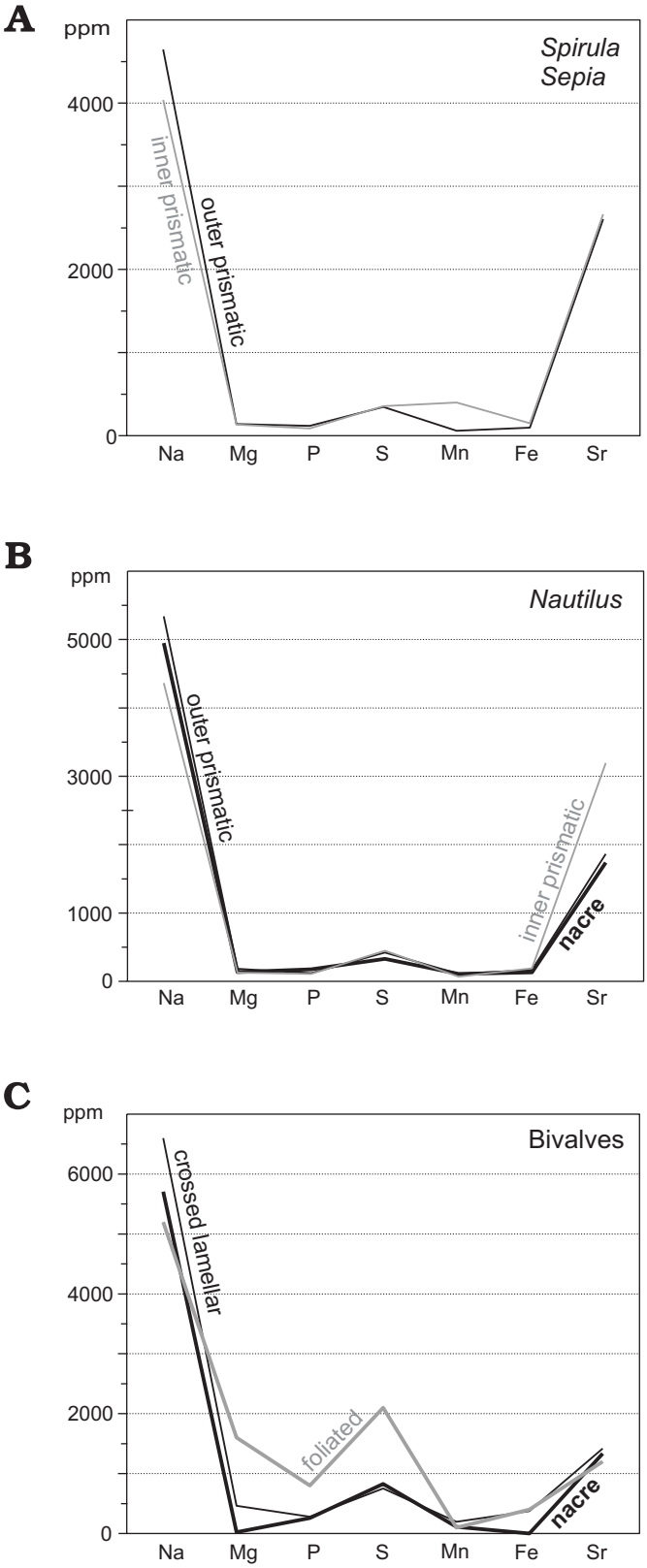

Fig. 4. Minor element contents (in ppm) in Recent shells. **A**. Average compositions of inner prismatic and outer prismatic aragonite layers in *Sepia* and *Spirula*. **B**. Average compositions of inner prismatic, nacreous and outer prismatic aragonite layers in *Nautilus macromphalus*. **C**. Average compositions of crossed lamellar aragonite layer in gastropods; in the nacreous aragonite layer in *Pinna nobilis*, and foliated calcite layer in *Pecten*.

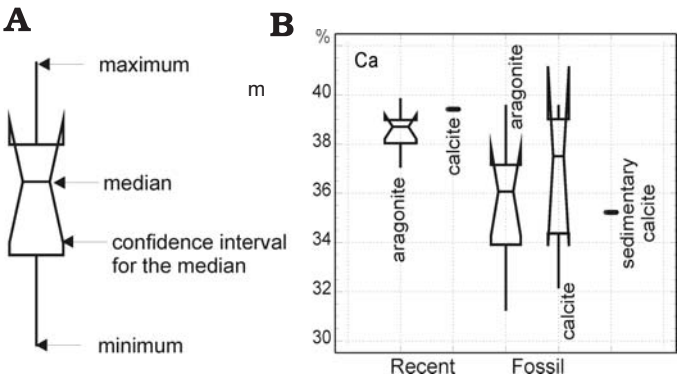

Fig. 5. Box and whisker plots based on the chemical compositions of the shells. **A**. Explanation of the box and whisker plot. **B**. Box and whisker plot for Ca in Recent and fossil shells, and sedimentary calcite.

shell of *Pecten* has a foliated microstructure (Fig. 2E) (Taylor et al. 1969), and the selected gastropod shells have a crossed lamellar layer composed of aragonite (Fig. 2F) (Boggild 1930).

Fossil samples.—Details of the microstructure of *Goniocamax* are shown in Fig. 3A–F. The diameter of the posterior calcite section of the rostrum is greater than that of the anterior aragonite part, and the calcite–aragonite boundary transects the rostra growth lines (Figs. 1A, 3A, B). The coarse calcite prisms of the posterior part are similar to those of entirely calcite belemnites, but in some places, the calcite prisms are thin (Fig. 3C). Growth lines are not clearly visible, and sectors are absent (Barskov et al. 1997).

The inner rostral surface of the alveolar part is undulated and shows regular longitudinal bands. In transverse sections, these bands appear as sectors that progressively disappear and are absent in the outer part of the rostrum (Fig. 3D, E).

In the anterior, thin prisms of aragonite are arranged in concentric growth lines (Fig. 3F). In the main part of the samples, the calcite region appears more dense and compact than the aragonite zone, and the aragonite shell layers are easily separated by "desquamation".

The most abundant structure in ammonites is the aragonite nacreous layers (Fig. 3G). In the Piasina ammonites, this layer is variably altered and the nacreous structure is not easily identifiable at low magnifications. The thin aragonite prismatic layers are also modified by the diagenetic processes (Barskov et al. 1997).

The microstructures of the gastropod shells show clear evidence of alteration with the crossed lamellar layers only locally being preserved and identifiable (Fig. 3H). First and second order units are sometimes visible. Inoceramid shells are usually composed of two layers: an inner aragonite nacreous layer and an outer prismatic one. The inner nacreous layer is present in the Piasina samples, with an altered ultrastructure (Fig. 3I). Additionally, the foliated layer of the *Pecten* shell is altered.

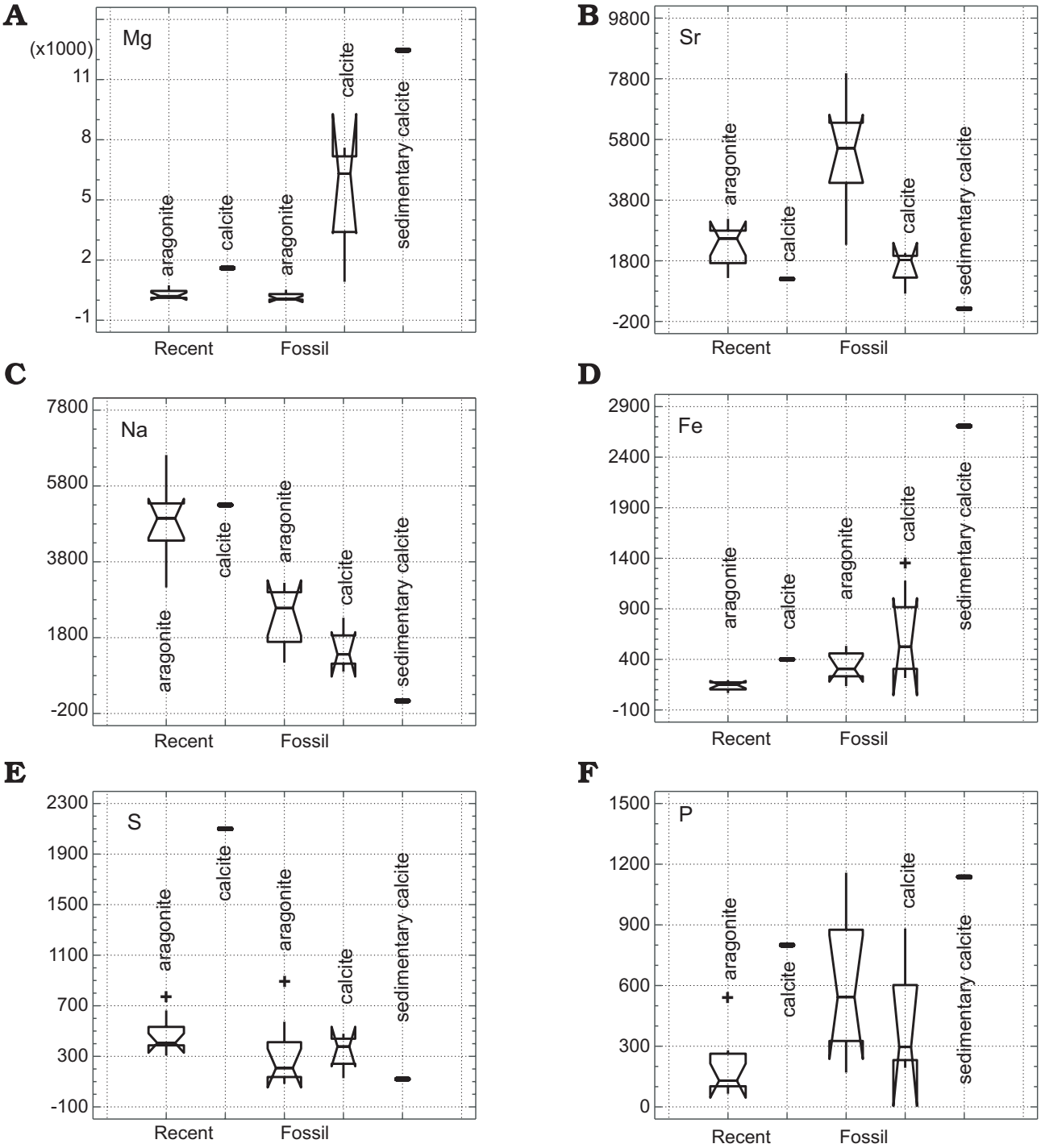

Fig. 6. Box and whisker plots for selected minor elements in Recent and fossil shells, and sedimantary calcite. Details of analysed samples are given in the section "Materials and methods". Plots are for magnesium Mg (**A**), strontium Sr (**B**), sodium Na (**C**), iron Fe (**D**), sulphur S (**E**), and phosphorus P (**F**). Recent samples: left part of the graph; fossil samples: right part of the graph.

Chemical composition

Average concentrations and coefficients of variation for both major and minor elements in the Recent shells are given in Table 1, with those of fossil samples presented in Table 2. Some elements are below the detection limit for the microprobe, particularly for the Recent shells, but this information is important because it allows for a direct comparison with fossil samples.

Recent samples.—All the layers in the Recent aragonite shells are characterized by relatively low Sr and S contents (Table 1, Fig. 4). There are no clear compositional differences between either the various layers in the cephalopods

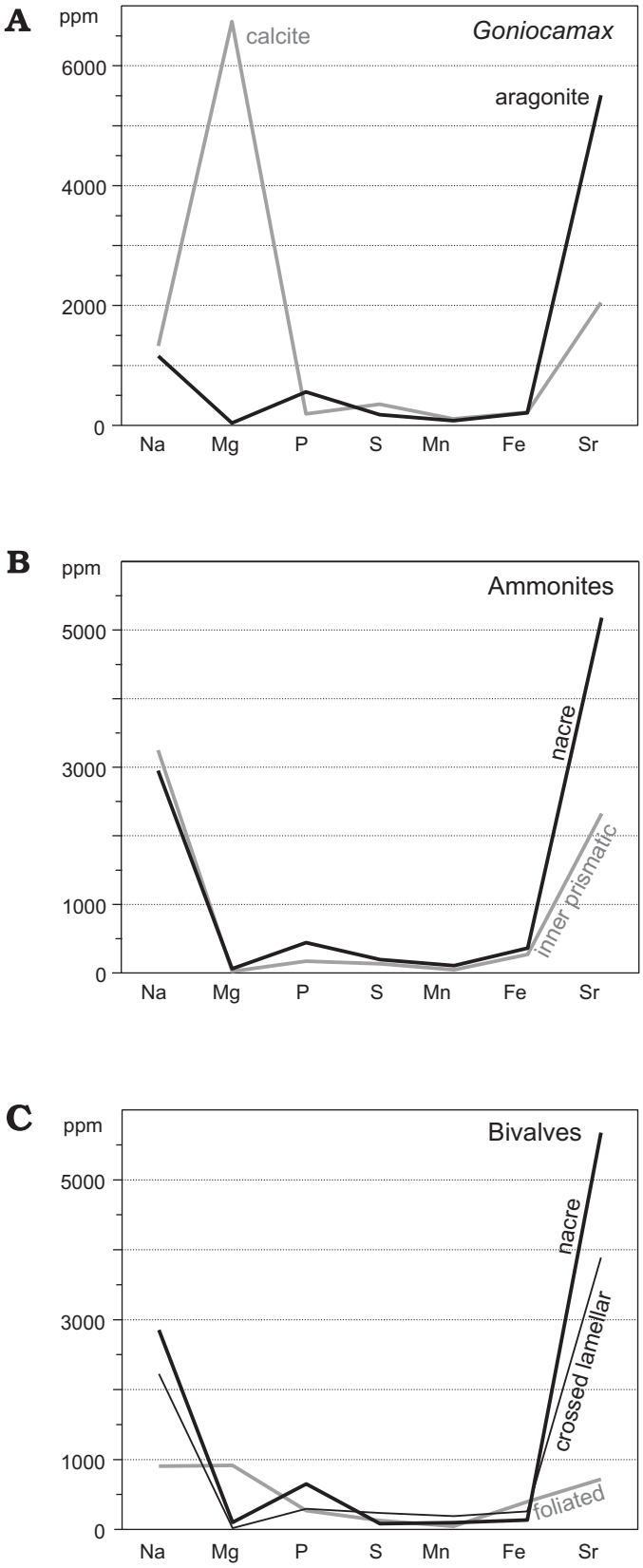

Fig. 7. Minor element contents (in ppm) in fossil shells. **A**. Average compositions of aragonite and calcite in *Goniocamax*. **B**. Average compositions of inner prismatic and nacreous layers in ammonites. **C**. The compositions of a crossed lamellar aragonite layer in a gastropod; a nacreous aragonite layer in an inoceramid shell, and a foliated calcite layer in *Pecten*.

(Fig. 4A, B), or between cephalopods, gastropods and bivalves (Fig. 4C). The Recent aragonite shells are essentially homogeneous in composition as can be seen that no outliers are present from the box and whisper plots for Ca (Fig. 5B) and Mg, Sr, Na, and Fe (Fig. 6). The only outlier seen is for P in the crossed lamellar layer of the gastropods box (Fig. 6). The outlier for S corresponds to the nacreous layer of *Pinna*, but this low value is close to the microprobe detection limit. The calcite shell of *Pecten* has high Mg and S contents. It is noticeable that the Sr content of the foliated calcite layer is similar to that of the aragonite nacreous layer of *Pinna*; however, in general the minor element contents of the Recent aragonite and calcite are statistically different according to the box and whisker plots (at the 95% confidence level).

Fossil samples.—The calcite component of the three rostra of *Goniocamax* has relatively high Mg contents (Table 2, Fig. 7A). Two of these rostra are enriched in P and Fe, but transversal and longitudinal sections show that the distributions of these elements are heterogeneous. Box and whisker plots show a wide variation in Mg, Fe (an outlier: *Goniocamax*) and P in the fossil calcite components (Fig. 6). The Ca content is also variable (Fig. 5B). The aragonite component of the three rostra of *Goniocamax* has relatively high Sr and low Na contents (Table 2, Fig. 7A), whereas Fe and P are variable. An aragonite *Goniocamax* is shown as an outlier for S contents (Fig. 6).

The element distribution maps were performed on the rostrum and show S and Fe are relatively homogenously distributed. The maps for Sr and Mg however, clearly distinguish the boundary between the aragonite and calcite components of the rostrum (Fig. 8A, B). Additionally, the Sr and Mg maps illustrate the presence of growth lines: Sr in the aragonite part, and Mg in the calcite part. These growth lines are not visible in the Fe map (Fig. 8C), but can be seen in the S map (Fig. 8D) in both the calcite and aragonite components.

The nacreous layers of some ammonites and the inoceramid shell are also enriched in Sr relative to the prismatic layers (Fig. 7B, C); in the case of inoceramid, this enrichment is irregular, and is coupled with an enrichment in P (Table 2, Fig. 7C).

Other notable differences are: the gastropod shell has relatively low Na high Sr contents (Fig. 7C); the foliated calcite layer of the *Pecten* shell has low Mg, S, and Sr contents (Table 2, Fig. 7C), and the fossil calcite and aragonite differ in their Sr and Mg contents (Fig. 6). They also clearly differ in that calcite is present in the ammonite chambers (Table 2, Fig. 6).

Comparison between Recent and fossil shells.—The box and whisker plot for Ca shows that the fossil samples, both aragonite and calcite, are more variable in Ca content than the Recent ones (Fig. 5B), and that the fossils are generally depleted in Ca. Both Recent and fossil calcite samples have relatively higher Ca contents than the corresponding aragonite samples.

In terms of the minor elements, fossil calcite samples are depleted in Na, S, and P relative to their Recent counterparts,

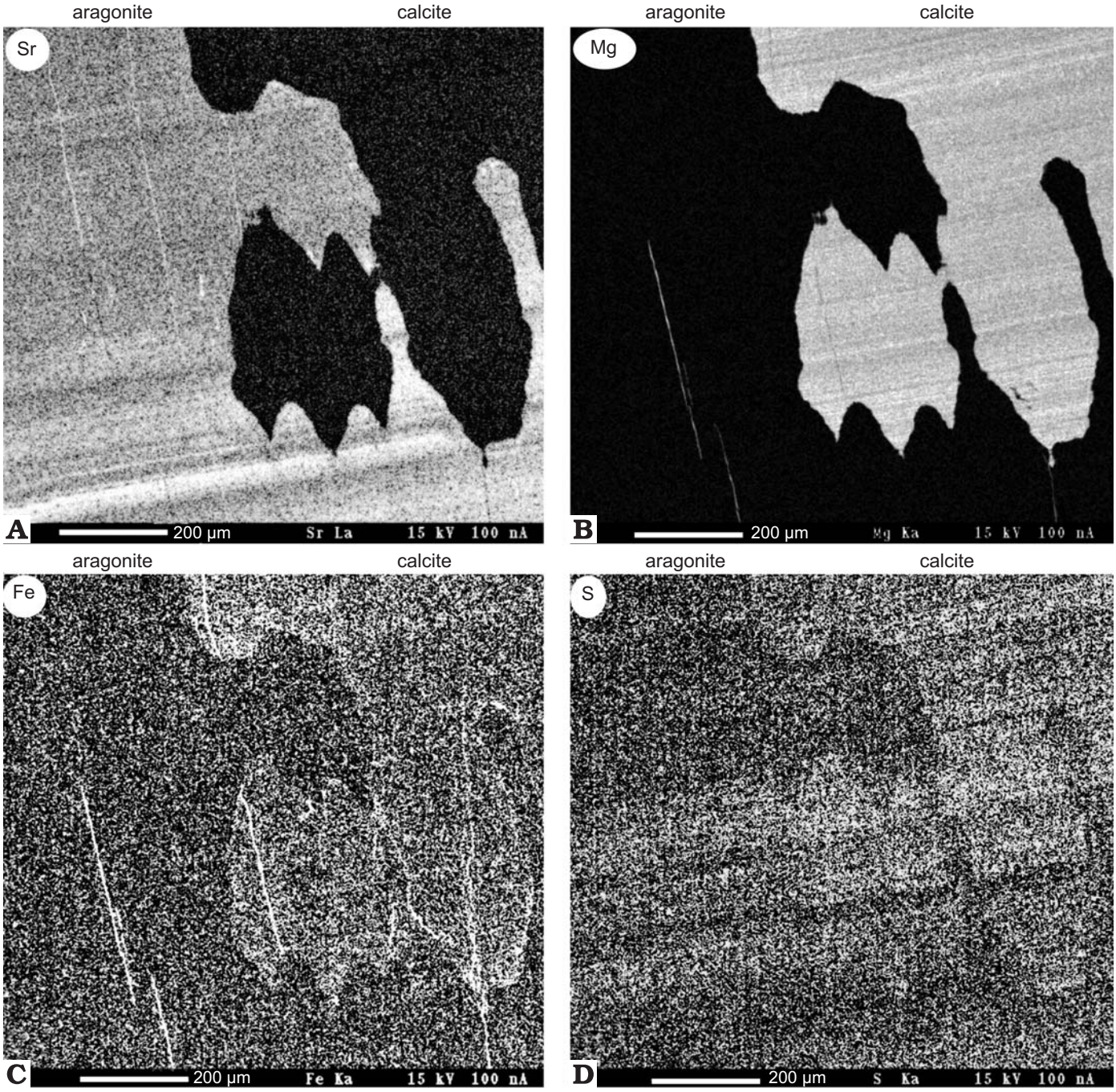

Fig. 8. Element distribution maps for Sr (**A**), Mg (**B**), Fe (**C**), and S (**D**) across the aragonite/calcite boundaries in *Goniocamax* sp. from the Turonian of N Siberia.

but they are enriched in Mg and Fe (Fig. 6). Recent and fossil aragonites differ in their minor element compositions, particularly for Na, Sr, Fe, and P (Fig. 6), with Mg and S showing least variability. These plots also illustrate the greater range of variation in the fossil aragonite samples compared with Recent samples for all the minor elements with the exception of Mg. This small variation in Mg for fossil aragonite contrasts with the observed large variation for this element in the fossil calcite samples. The range of variation of the fossil calcite differs according to the element, being small for Sr, and large for Mg, Fe, and P.

Two principal component analyses were undertaken on the data sets: the first included all the Recent and fossil samples (Figs. 9, 10); in the second were added data for the infilling calcite and enclosing calcareous sediment (Fig. 11).

(1) Recent and fossil shells (22 shells): The highest correlation coefficient (0.72) is between P and Fe. The first principal axis (Fig. 9) contains 36.3% of the total variance, axis 2 = 24.1% and axis 3 = 19.3%. The first principal component calculates high negative loadings to P, Fe, and Sr opposed to Na (Fig. 9A). The second principal component gives high negative loadings to S, Ca, and Fe, and positive loadings to Sr. The

third principal component gives high negative loading to Mg opposed to Sr. The Recent and fossil samples are clearly separated on the basis of the principal component plots (Fig. 9A, 10), mainly in terms of their Na and Ca (higher in calcite) and P, Fe, and Sr (higher in aragonite). The total area for the fossil samples is larger than the Recent samples (Fig. 9A), illustrating the more compositional variability in the fossil samples. When the data are analysed according to sample mineralogy (Fig. 9B), there is less distinction between the two groups (i.e., calcite and aragonite). Calcite samples are enriched in S and

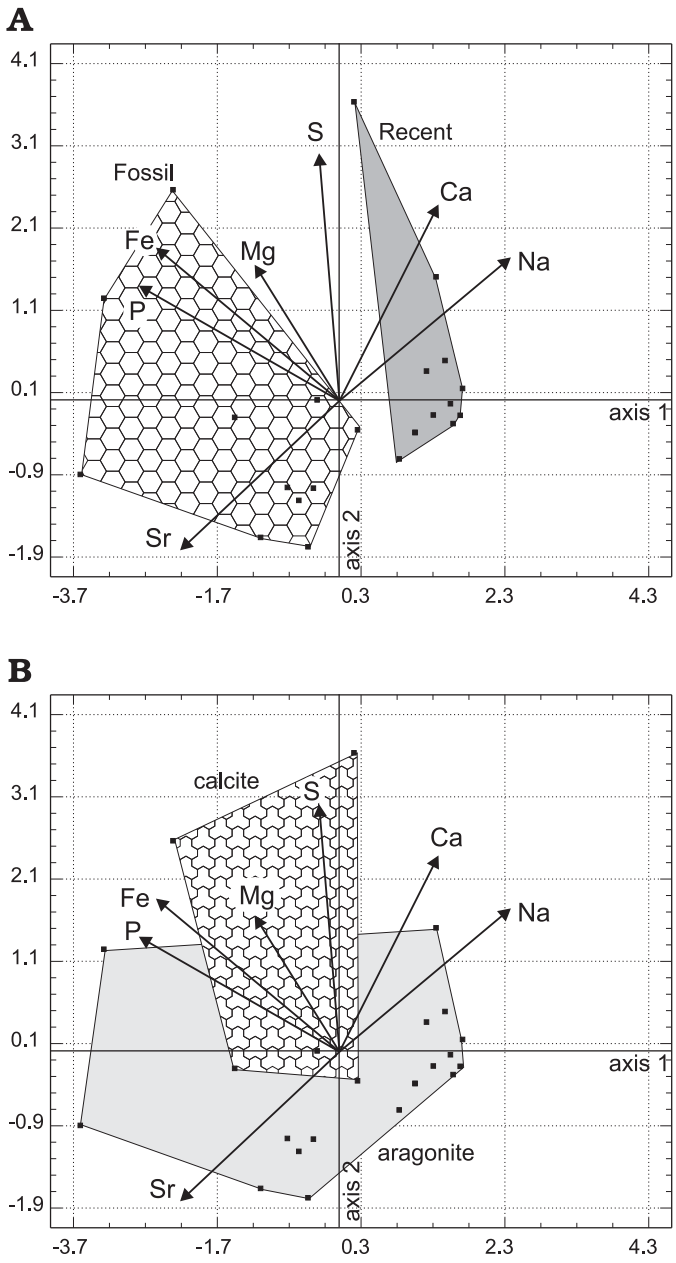

Fig. 9. Principal component plots based on the chemical compositions of the Recent and fossil shells. **A**. Samples are grouped according to their age, with Recent shells having relatively high Ca and Na contents, and low Fe, P, and Sr contents. **B**. Samples are grouped according to their mineralogy in terms of calcite and aragonite. Calcite samples have relatively high Mg, S, and Ca contents, and aragonite samples have higher Sr contents.

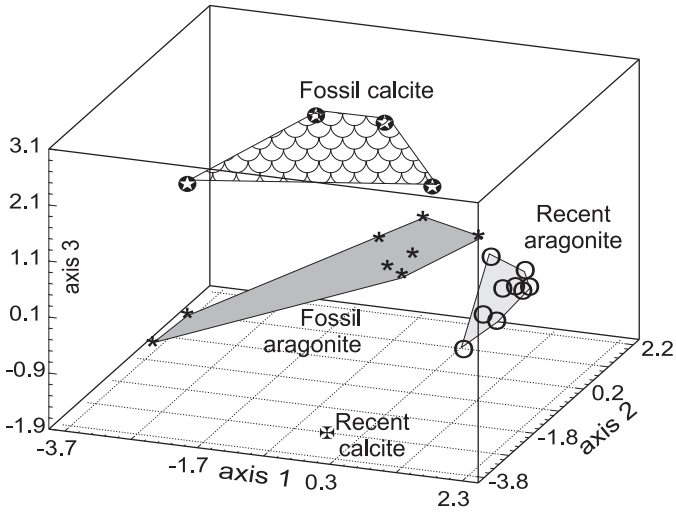

Fig. 10. 3D principal component plots based on the chemical compositions of the Recent and fossil shells. Axis 1 has high negative loadings corresponding to P, Fe, and Sr, with a positive Na loading. Axis 2 has high negative loadings corresponding to S, Ca, and Fe, and a positive Sr loading. Axis 3 has a high negative loading corresponding to Mg and a positive Sr loading. Recent and fossil calcites are separated according to axis 3, whereas Recent and fossil aragonites are separated according to axis 1.

Mg, whereas aragonite samples have higher Sr contents, but P and Fe are not good discriminators. The 3-D representation of the same data (Fig. 10) shows that the recent calcite sample *Pecten* (one sample) and the fossil calcite shells plot on opposing sides of the fossil aragonite samples. This recent *Pecten* sample is different from the fossil *Pecten* in its low Na, Mg, S, and Sr contents, and different also from the fossil calcite samples in having lower Mg and Sr contents. Moreover, the area for recent aragonite samples is smaller than that for the fossil aragonites, indicating again the recent samples are more homogenous than the fossil samples.

(2) Shells and non-biogenic sediments (24 samples): The highest correlation coefficient (0.98) is between P and Fe. The first principal axis contains 56.9% of the total variance, axis 2 = 17.8% and axis 3 = 14.2%. The first principal component gives high negative loadings for P and Fe, and positive loadings for Ca (Fig. 11). The second principal component gives high negative loadings for Sr and positive loadings for Mg. The chemical compositions of the Recent and fossil shells are clearly different from both those of the calcite in the ammonite chambers, and from the sediment.

Discussion

The Piasina fossils.—Shells such as ammonites, the inoceramid nacreous layer and the crossed lamellar layer in bivalves and gastropods are composed of aragonite; despite having various microstructures, the nuculid shells are also composed of aragonite; the main layer of the *Lopatinia* shells (Arcoida) is also composed of aragonitic crossed lamellar

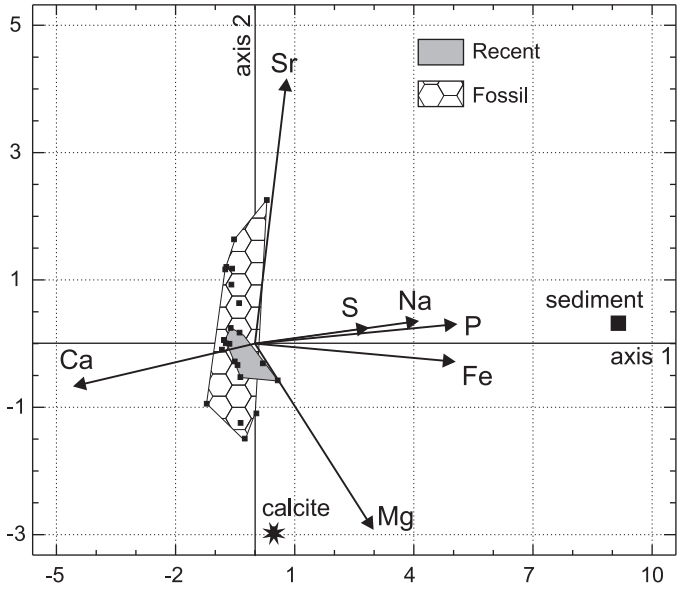

Fig. 11. Principal component plots based on the chemical compositions of the Recent and fossil shells, sediments and sedimentary calcite. Sedimentary calcite (labelled "calcite" in the diagram) is clearly separated from the Recent and fossil shell calcites.

structures; the foliated shell of *Pecten* is primarily calcite. The key question is whether the fossil belemnitid rostra were originally calcite or aragonite.

A comparison of shells with undisputed mineralogy shows that the microstructures of the aragonite shells have been affected by diagenesis (Barskov et al. 1997), with the nacreous layer of ammonites and inoceramids, and the crossed lamellar layers of the gastropods all being modified. However, these aragonitic shells are preserved in aragonite. The heterogeneity of the preservation of the aragonite in these concretions is demonstrated by the fact that the nuculids and *Lopatinia* shells are composed of "white calcite" (Teys et al. 1978). The calcite layer of the fossil *Pecten* also shows the effects of diagenetic alteration.

The chemical compositions confirm these observations, as the Sr contents of fossil aragonites are too high for molluscs, and the Na and Ca contents too low. However, the minor elements S and Mg do not appear to have been significantly affected during diagenesis. Another observation in favour of the aragonite having been modified is that two rostra of *Goniocamax* have relatively high P and Fe contents (Table 2), these two elements being indicators for diagenetic alteration during this fossilization process. Individual *Goniocamax* rostra display variable degrees of compactness and density illustrated best in the growth layers and overall microstructure. Where the shell has a friable appearance, higher P and Fe contents are seen (Table 2). However, where growth layers are contiguous and the microstructure has a more compact and dense appearance, P and Fe contents are significantly lower. Thus, there is a clear correlation between the presence and amount of the extraneous diagenetic elements and the microstructure of the aragonite. The calcite components of *Goniocamax* appear more compact than the aragonite, but contain also lacunae that can act as pathways for fluid transport through capillary action. Of note also is that, within the same rostra, there is an enrichment of P and Fe in regions of both calcite and aragonite, indicating they have been subjected to diagenesis. Additonally, there is no correlation observed between the Mg and Fe contents. However, the diagenetic process must have been relatively complex as illustrated by the fact that three *Goniocamax* samples have high Fe contents, two being calcitic, the third being aragonitic, whereas one calcitic *Goniocomax* has low contents of Fe.

Stable isotope data for oxygen and carbon from several studies provide additional information on the diagenetic alteration of these shells. The $\delta^{18}O$ compositions of both the aragonite and calcite of *Goniocamax* are similar (Teys et al. 1978). However, these values are negative, whereas they are mainly positive in the Recent *Sepia* (Bettancourt and Guerra 1979). The $\delta^{18}O$ composition of the aragonite layers in ammonite is more negative than those of *Goniocamax*, and strongly differs from that of the Recent adult *Nautilus* (0.05 to 2 for *Nautilus pompilius*: Cochran et al. 1981; Oba et al. 1992). The $\delta^{13}C$ values are different in the calcite and aragonite components of *Goniocamax* (Teys et al. 1978), but the aragonite values are similar to those of the Recent *Sepia*. The $\delta^{13}C$ values of the Piasina ammonites range between –4.27 and 0.50‰, whereas those of the Recent *Nautilus* have a more constrained range of between –0.8 to 1.2‰ (Cochran et al. 1981). Thus, the isotopic data indicate that both aragonite and calcite from the *Goniocamax* rostra are altered.

The calcite comprising the fossil *Pecten* has been modified, and is depleted in Na, Sr, Mg, and S. The chemical composition of the calcite filling the ammonite chamber is clearly different from that of the shells (Table 2, Fig. 10), but both have high Fe and P contents. However, the Mn contents infilling calcite and sediment are significantly higher than in either fossil calcites or aragonites.

Thus, a combination of microstructural, chemical, and isotopic data suggest that both the aragonite and calcite have been altered, and indeed the biogenic rostral aragonite of *Goniocamax* has been partly replaced by precipitation of secondary aragonite during diagenesis.

Broader palaeo-environmental implications.—Some authors have reported systematic intra-sample differences in Recent bivalves for some trace elements, including Mg and Sr, that are interpreted as resulting from either seasonal, or ontogenical variations (e.g., Putten et al. 2000; Jiménez-Berrocoso et al. 2004). However, the electron probe techniques employed in this study would not have been sensitive enough to identify any minor variations in these elements at the low concentration levels present in Recent bivalve samples.

Many palaeo-environmental reconstructions, including palaeosalinities have been based on minor element contents of molluscan shells. Brand (1986) used Sr/Na ratios in aragonite

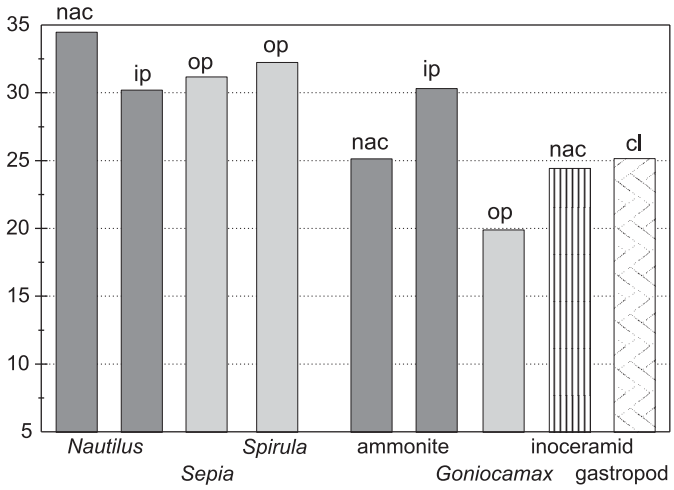

Fig. 12. Water salinities (in ppt) calculated from Recent and fossil aragonite samples. Abbreviations: op, outer prismatic layer; ip, inner prismatic layer; nac, nacreous layer; cl, crossed lamellar layer.

shells to construct palaeosalinities, and an application of this model has been attempted here (Fig. 12). The salinities calculated from the Recent samples from New Caledonia are in accordance with the known values of the water salinity in this region, i.e., between 34 and 35.7 ppt near the surface, and 34.6 ppt 500 m below the surface. However, palaeosalinity values calculated from the same fossil samples of the Piasina River, vary between 19.9 and 30.3 ppt, with the lowest value corresponding to the aragonite component of *Goniocamax*. Additionally, there are large calculated differences between the inner prismatic and nacreous layers of the fossil samples. Thus, palaeosalinity calculations do not appear to work in samples from the Piasina site, as diagenesis has significantly altered the original chemical composition of the samples.

Two diagenetic stages have been observed in Jurassic bivalves (Hendry et al. 1995). The early neomorphic calcite contains negligible amounts of Fe, Mn, and Mg, while late neomorphic calcite has high Mg, Fe, and Mn contents. According to these authors, this two stage diagenetic process contradicts previous hypotheses that the aragonite–calcite change is a one-step process. Moreover, Hendry et al. (1995) have noticed that "… the early stage of aragonite replacement was initiated at numerous reaction sites distributed throughout the shells, rather than following a continuous neomorphic front". Microstructural observations of the *Goniocamax* samples have shown that the boundary between calcite and aragonite is not regular. Hendry et al. (1995) also concluded that "... calcitization ... was principally controlled by the distribution of the skeletal organic matrix".

The processes leading from biogenic aragonite to secondary aragonite, or from biogenic aragonite to calcite are not well known. The presence and high diversity of the intercrystalline and intracrystalline organic matrices in mollusc shells are well established since the pioneering studies of Grégoire et al. (1955) and Grégoire (1969). Only a few shell layers have been studied, but these matrices are acidic glycoproteins, and are taxonomically related (Lowenstam and Weiner 1989; Dauphin 2001a). More recently, it has been shown that the sulphur present in the shells is not inorganically-bound S, but organic S, the main part of which being associated with sulphated sugars and not S amino acids (Dauphin 2001b; Dauphin et al. 2003a, b). Although the role of the quantity and composition of the organic matrix in diagenetic processes is still unknown, results from the Cretaceous Piasina River (Northern Siberia) and Triassic Turkish fossils (see Cuif et al. 1977) indicate that these matrices may have played a key role, and it is no longer possible to neglect the organic matrix. Thus, such samples show that not only is the usual control of the mineralogy for isotopic based palaeo-environmental reconstructions insufficient, but that the examination of the microstructures has to be correlated with minor element contents. The fact that some palaeotemperatures are plausible does not mean that they are those of the living animals, and may simply reflect a diagenetic overprint modifying the original composition, and thus distorting any calculated palaeotemperature.

Acknowledgments

This research was supported by The International Association for the Promotion of Co-operation with Scientists from the New Independent States (NIS) of the Former Soviet Union grant 93-1494, and by the Improving Human Potential, European Union Fellowship Program for YD to visit the Natural History Museum, London. We are grateful for comments from the reviewers, especially Idoia Rosales (Instituto Geológico y Minero, Madrid, Spain) that have improved the manuscript.

References

Bandel, K., Engeser, T., and Reitner, J. 1984. Die Embryonalentwicklung von *Hibolites* (Belemnitida, Cephalopoda). *Neues Jahrbuch für Geologie und Paläontologie, Abhandlungen* 167: 275–303

Barskov, I.S. Kiyashko, S.I., Dauphin, Y., and Denis, A. 1997. Microstructures des zones calcitiques et aragonitiques des rostres de *Goniocamax* (Belemnitida, Turonien, Sibérie du Nord). *Geodiversitas* 19: 669–680.

Barskov, I.S. 1972. Microstructure of the skeletal layers of belemnites compared with external shell layers of other Mollusks. *Paleontological Journal* 4: 492–500.

Barskov, I.S. 1973. Microstructure of the skeletal layers of *Sepia* and *Spirula* compared with the shell layers of other Mollusks. *Paleontological Journal* 3: 286–294.

Bettencourt, V. and Guerra, A. 1999. Carbon- and oxygen isotope composition of the cuttlebone of *Sepia officinalis*: a tool for predicting ecological information? *Marine Biology* 133: 651–657.

Boggild, O.B. 1930. The shell structure of the molluscs. *Det Kongelige Danske Videnskabernes Selskabs Skrifter, Naturvidenskabelig og Mathematisk Afdeling* 9: 231–326.

Brand, U. 1986. Paleoenvironmental analysis of Middle Jurassic (Callovian) ammonoids from Poland: trace elements and stable isotopes. *Journal of Paleontology* 60: 293–301.

Cochran, J.K., Rye, D.M., and Landman, N.H. 1981. Growth rate and habitat of *Nautilus pompilius* inferred from radioactive and stable isotope studies. *Paleobiology* 7: 469–480.

Cuif, J.P., Dauphin, Y., Denis, A., Gaspard, D., and Keller, J.P. 1980. Continuité et périodicité du réseau organique intraprismatique dans le test de *Pinna muricata* Linné (Lamellibranche). *Comptes Rendus hebdomadaires de l'Académie des Sciences de Paris (sér. D)* 290: 759–762.

Cuif, J.P., Dauphin, Y., and Lefèvre, R. 1977. Rapport de la localisation du strontium, magnésium et sodium avec la minéralogie et la microstructure de trois rostres d'Aulacocerida triasiques. *Comptes Rendus hebdomadaires de l'Académie des Sciences de Paris (sér. D)* 285: 1033–1036.

Cuif, J.P., Denis, A., and Raguideau, A. 1983. Observations sur les modalités de mise en place de la couche prismatique du test de *Pinna nobilis* L. par l'étude des caractéristiques de la phase minérale. *Haliotis* 13: 131–141.

Dauphin, Y. 1976. Microstructure des coquilles de Céphalopodes. I – *Spirula spirula* (L.) (Dibranchiata, Decapoda). *Bulletin du Museum National d'Histoire Naturelle de Paris (3èm sér.)* 382, *Sciences de la Terre* 54: 197–238.

Dauphin, Y. 1981. Microstructures des coquilles de Céphalopodes. II – La seiche (Dibranchiata, Decapoda). *Palaeontographica A* 176: 35–51.

Dauphin, Y. 1983. Microstructure du phragmocône du genre triasique *Aulacoceras* (Cephalopoda – Coleoidea) – remarques sur les homologies des tissus coquilliers chez les Céphalopodes. *Neues Jahrbuch für Geologie und Paläontologie, Abhandlungen* 165: 418–437.

Dauphin, Y. 1986. Microstructure des coquilles de Céphalopodes: la partie apicale de *Belopterina* (Coleoidea). *Bulletin du Museum National d'Histoire Naturelle de Paris (3èm sér.*) 8, C1: 53–75.

Dauphin, Y. 1987. Les microstructures des rostres de Céphalopodes. VIII – apport de la microanalyse localisée pour l'interprétation de l'état diagénétique des rostres d'Aulacocéridés (Trias – Turquie). *Palaeontographica A* 199: 217–231.

Dauphin, Y. 1988. Diagenèse aragonite–calcite chez les Céphalopodes coléoïdes: exemples des rostres d'*Aulacoceras* (Trias de Turquie) et de *Belopterina* (Eocène de France). *Bulletin du Museum National d'Histoire Naturelle de Paris* (*4èm sér.*) 10, C2: 107–135.

Dauphin, Y. 2001a. Caractéristiques de la phase organique soluble des tests aragonitiques des trois genres de céphalopodes actuels. *Neues Jahrbuch für Geologie und Paläontologie, Monatshefte* 2: 103–123.

Dauphin, Y. 2001b. Comparative studies of skeletal soluble matrices from some Scleractinian corals and Molluscs. *International Journal of Biological Macromolecules* 28: 293–304.

Dauphin, Y. and Cuif, J.P. 1980. Implications systématiques de l'analyse microstructurale des rostres de trois genres d'Aulacocéridés triasiques (Cephalopoda – Coleoidea). *Palaeontographica A* 169: 28–50.

Dauphin, Y., Cuif, J.P., Doucet, J., Salomé, M., Susini, J., and Williams, C.T. 2003a. *In situ* chemical speciation of sulfur in calcitic biominerals and the simple prism concept. *Journal of Structural Biology* 142: 272–280.

Dauphin, Y., Cuif, J.P., Doucet, J., Salomé, M., Susini, J., and Williams, C.T. 2003b. *In situ* mapping of growth lines in the calcitic prismatic layers of mollusc shells using X-ray absorption near-edge structure (XANES) spectroscopy at the sulphur edge. *Marine Biology* 142: 299–304.

Engeser, T. and Reitner, J. 1983. *Chitinobelus acifer* Fischer 1981, ein Belemnoteuthide (Coleoidea) mit Epirostrum. *Neues Jahrbuch für Geologie und Paläontologie, Abhandlungen* 165: 496–501.

Grégoire, C. 1969. Further studies on structure of the organic components in mother-of-pearl, especially in Pelecypods. *Bulletin de l'Institut Royal de Sciences naturelles de Belgique* 36: 1–22.

Grégoire. C., Duchateau, G., and Florkin, M. 1955. La trame protidique des nacres et des perles. *Annales de l'Institut Océanographique* 31: 1–36.

Hendry, J.P., Ditchfield, P.W., and Marshall, J.D. 1995. Two-stage neomorphism of Jurassic aragonitic bivalves: implications for early diagenesis. *Journal of Sedimentary Research A* 65: 214–224.

Jeletzky, J.A. 1966. Comparative morphology, phylogeny and classification of fossil Coleoidea. *University of Kansas Paleontological Contributions, Mollusca* 7: 1–162.

Jiménez-Berrocoso A., Zuluaga M.C., and Elorza, J. 2004. Minor- and trace-element intra-shell variations in Santonian inoceramids (Basque-Cantabrian Basin, northern Spain): diagenetic and primary causes. *Facies* 50: 35–60.

Kostak, M., Cech, S., Ekrt, B., Mazuch, M., Wiese, F., Voigt, S., and Wood, C.J. 2004. Belemnites of the Bohemian Cretaceous Basin in a global context. *Acta Geologica Polonica* 54: 511–533.

Lowenstam, H.A. and Weiner, S. 1989. *On Biomineralization*. 324 pp. Oxford University Press, Oxford.

Makowski, H. 1962. La faune callovienne de Lukow en Pologne. *Palaeontologia Polonica* 4: 1–64.

Muller-Stoll, H. 1936. Beitrage zur Anatomie der Belemnoidea. *Nova Acta Leopoldina (NS)* 4: 159–226.

Mutvei, H. 1964. On the shells of *Nautilus* and *Spirula* with notes on the shell secretion in non cephalopod molluscs. *Arkiv för Zoologi* 16: 221–278.

Naydin, D.P. [Najdin, D.P.], Barskov, I.S., and Kiyachko, S.I. [Kijačko, S.I] 1987. Aragonitic and calcitic composition of the belemnitid rostra from the Upper Cretaceous of the western Taymyr: stable isotopic composition of oxygen and carbon [in Russian]. *Paleontologičeskij žurnal* 3: 3–8.

Oba, T., Kai, M., and Tanabe, K. 1992. Early life history and habitat of *Nautilus pompilius* inferred from oxygen isotope examinations. *Marine Biology* 113: 211–217.

Putten, E.V., DeHairs, F., Keppens, E., and Baeyens, W. 2000. High resolution distribution of trace elements in the calcite shell layer of modern *Mytilus edulis*: environmental and biological controls. *Geochimica et Cosmochmica Acta* 64: 997–1011.

Reitner, J. and Engeser, T. 1982. Phylogenetic trends in phragmocone-bearing coleoids (Belemnomorpha). *Neues Jahrbuch für Geologie und Paläontologie, Abhandlungen* 164: 156–162.

Spaeth, C. 1971. Aragonitische und calcitische Primarstrukturen im Schalenbau eines belemniten aus der englischen Unterkreide. *Paläont. Zeitschrift* 45: 33–40.

Taylor, J.D., Kennedy, W.J., and Hall, A. 1969. The shell structure and mineralogy of the Bivalvia. Introduction. Nuculacae—Trigonacae. *Bulletin of the British Museum of Natural History, Zoology* 3: 1–125.

Teys, R.V., Kiseleskiy, M.A., and Naydin, D.P. 1978. Oxygen and carbon isotopic composition of organogenic carbonates and concretions in the Late Cretaceous rocks of Northwestern Siberia. *Geochemistry International* 15: 74–81.